Nuclear Instruments and Methods in Physics Research B 267 (2009) 2050–2053

Contents lists available at ScienceDirect

Nuclear Instruments and Methods in Physics Research B

journal homepage: www.elsevier.com/locate/nimb

Aperture edge scattering in focused MeV ion beam lithography and nuclear microscopy: An application for the GEANT4 toolkit

S. Gorelick *, Harry J. Whitlow

Department of Physics, University of Jyväskylä, P.O. Box 35 (FL), FIN-40014, Finland

ARTICLE INFO

Available online 13 March 2009

PACS:
24.10.Lx
41.85.Si
41.85.Ja
68.49.Sf
79.20.Rf
87.56.–J

Keywords:
MeV ion scattering
Monte-Carlo
Edge scattering
GEANT4
Aperture
Slit

ABSTRACT

Collimators are widely used to define MeV ion beams. Recent studies have shown the capability of combinations of collimators and lenses to define beams of MeV ions with sub-100 nanometre dimensions. Such nanometre beams have potential applications in MeV ion beam lithography, which is the only maskless technique capable of producing extremely high aspect ratio micro- and nano-structrures, as well as in high resolution MeV ion beam based imaging. The ion scattering from the collimator-edges can be a resolution restricting factor in these applications. Scattering processes at edges are difficult to study using conventional simulation codes because of the complicated geometry. In this work we overview the possibilities and pitfalls in using the GEANT4 toolkit as a simulation tool for studying the behaviour of ions impinging onto, or in close proximity to aperture edges. Results from simulations of scattering of 2 MeV protons incident on a 5 mm in diameter cylindrical beam defining tungsten carbide (WC) aperture blade, such as used in nuclear micro- and nanobeams as object and scraper apertures, are presented. The bubble formation at the aperture edges due to the implantation of H was first believed to cause edge roughening and hence the beam quality degradation. The concentration profile of implanted H in a WC cylinder shows that the bubble formation is not likely to be the edge roughening factor, but rather other mechanisms of beam induced topographical changes such as ion beam induced morphological changes and cracking of hydrocarbons.

© 2009 Elsevier B.V. All rights reserved.

1. Introduction

There are numerous applications requiring small beam spots of MeV ions [1–5]. Typically, a beam from an accelerator is collimated by object slits. The collimated beam is then magnetically focused (demagnified) to form a small beam spot [1,2]. This method allows the beam to be focused into spots with sub-100 nm size [6]. In an alternative approach the beam is well-collimated by an aperture or a set of apertures eliminating the focusing step [7–13]. This method provides a number of advantages over the focused beam approach, among them is tolerance to poor beam energy stability and divergence and allows the use of high energy heavy ions, which are hard to focus because of their high magnetic rigidity.

Both methods, however, rely on defining the beam spot by collimating the broad beam from the accelerator. In this paper we consider the case where a lens system is used to produce a demagnified image of the object aperture. In this case the beam spot quality is mainly sensitive to energy spreading caused by scattering of protons from the aperture edges. In this preliminary work, using the GEANT4 toolkit, we investigated the edge erosion and edge scattering [14,15] by a cylindrical tungsten carbide (WC) roller bearing of the type commonly used as a beam defining slits in nuclear microscopy.

2. Details of simulation

The GEANT4 toolkit [16–18] was used to estimate the implantation profile of hydrogen in a WC cylinder and the extent of the edge scattering. GEANT4 is an object-oriented Monte-Carlo simulation tool written in C++ that provides comprehensive detector and physics modeling capabilities. GEANT4 was used rather than other conventional simulation programs (e.g. SRIM [19]) because of the possibility to track particles in a user-defined complex three-dimensional geometries. Furthermore, simulations on a micrometre scale [20] showed that GEANT4 is suitable to investigate the near-edge ion scattering. Ion processes, such as multiple scattering and energy loss via electronic and nuclear stopping, were simulated using the low energy EM physics package in GEANT4 [18,21]. The general particle source (GPS) was used to generate ion beams with the desired energy, angular and spatial distributions [22]. The *cut in*

* Corresponding author. Address: Laboratory for Micro- and Nanotechnology, Paul Scherrer Institut, 5232 Villigen-PSI, Switzerland. Tel.: +41 56 310 2574; fax: +41 56 310 2646.
E-mail address: sergey.gorelick@psi.ch (S. Gorelick).

0168-583X/$ - see front matter © 2009 Elsevier B.V. All rights reserved.
doi:10.1016/j.nimb.2009.03.074

range was set uniquely to 100 μm in all the simulations. To ensure reliable scattering in the slit, the maximum simulation step-length was set to 4 nm for 2 MeV protons in the WC cylinder (~1/4000 of the range of a 2 MeV proton in WC) [14,15].

3. Hydrogen implantation into a cylindrical edge

In nuclear microscopy, the size of the beam for prefocusing and the divergence of the beam are often defined by tungsten carbide (WC) roller bearings (13 mm long, 5 mm diameter) [23]. It has been noted that high fluences of irradiation caused degradation of the beam spot quality, i.e. the halo around the primary beam spot is enhanced. Fig. 1 shows the edge of the WC cylindrical slit exposed to the 2 MeV proton irradiation for a month or so. The edge is severely roughened by the impinging protons with a grain-like structure appearing on the slit surface. Bubble formation at the surface of the WC cylindrical blade by the implanted H could provide an explanation of the edge roughening. Using GEANT4, the spatial distribution of 2 MeV protons implanted in the cylindrical aperture edge was calculated (Fig. 2). In these simulations, the tip of the WC cylinder was irradiated with a fluence of 2 MeV protons. The WC cylinder was defined as a sensitive detector that could track the trajectories of individual protons transversing through it till either they were ejected from the edge or completely stopped within the slit. The positions of the ions that came to rest within the WC cylinder were saved in data files that were later analyzed. The results of such simulations are presented in Fig. 2. The maximum concentration of the implanted protons is located upstream of the aperture tip (Fig. 2(a)), with a lower concentration at the tip region of the WC cylinder (Fig. 2(b)). Even so, long lasting irradiations may build-up significant concentrations of implanted protons at the slit's near-surface region. Thus, for an incident beam current density of 1 μA cm^{-2}, the maximum of the implanted concentration will reach 10^{20} hydrogens cm^{-3} after about 20 days of constant irradiation, provided the implanted protons do not diffuse away. The implanted concentrations at the tip region of the WC cylinder are, however, about an order of magnitude smaller than in the upstream regions of the slit, but nevertheless the hydrogen concentrations at the tip can become significant even after short irradiations. The inclusion of the implanted hydrogen at the tip region of the WC cylinder will alter the density of the material in the edge of the slit. If the material relaxes (e.g. by void formation) the density and stopping force of protons traversing through the tip of the WC cylinder will decrease.

The structure of the damage on the WC cylindrical aperture blade induced by the irradiation (Fig. 1), however, does not obviously correlate with the calculated implanted profile. This suggests that other mechanisms are responsible for the slit-edge degradation, among them glancing angle sputtering, ion induced morphology changes and hydrocarbon deposition.

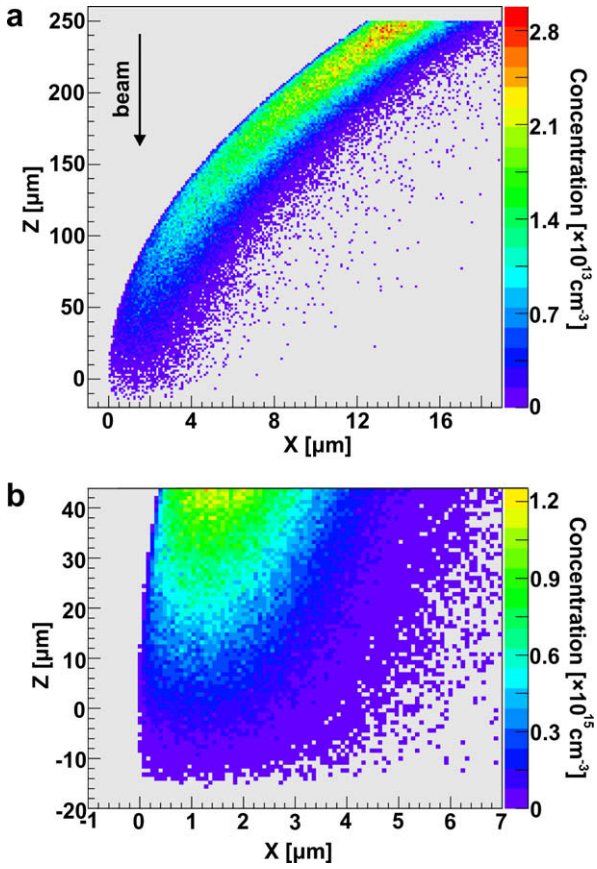


Fig. 2. Distribution of implanted protons in the WC cylinder resulting from irradiation of a fluence (number of protons per unit area directed perpendicular to the beam axis). The axis of the WC cylinder is in the *Y*-direction. The beam axis is in the – *Z*-direction. (a) Low fluence of 10^{11} protons cm^{-2}. (b) High fluence of 10^{14} protons cm^{-2} on the tip of the WC cylinder.

4. Scattering from a cylindrical edge

In the following study, the scattering of 2 MeV protons from the WC cylinder edge was investigated. In these simulations, a sample modelled as a sensitive detector was positioned downstream of the WC cylinder. Once a proton was ejected through the medium-vacuum boundary, the detector recorded the momentum directions of the proton, its energy and its entry coordinates into the detector. The data was saved into files for a later analysis. For edge scattering of protons originating from a point source and impinging on the WC cylinder at a certain distance from the tip we found that the protons incident at >0.5 μm from the slit's tip are ejected to large angles with respect to the beam incidence. Ions that have under-

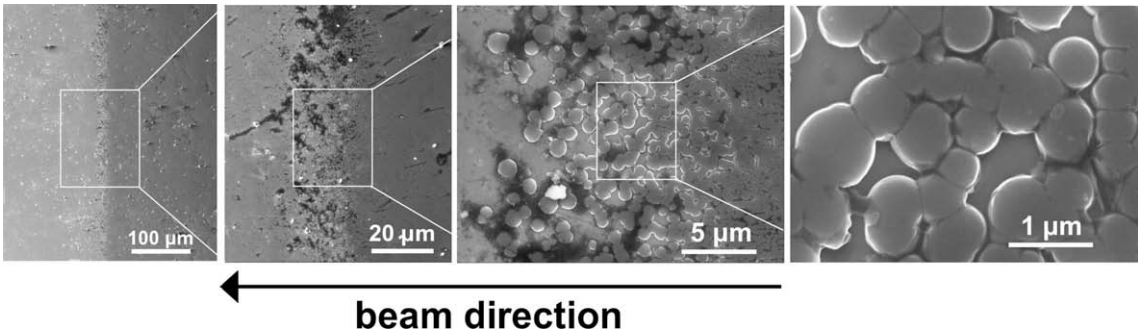


Fig. 1. Scanning electron microscope (SEM) images of WC cylinder edge degradation caused by long duration of 2 MeV proton irradiation. Sample courtesy of Frank Watt.

gone large angle scattering, or large energy loss do not contribute to the broadening of the focused beam, because they are filtered out by impingement on the scraper aperture or are removed by the dispersion of the magnetic lens. In the study of the scattering from the WC cylinder positioned at $X > 0$, only a 1 μm edge projected width of the slit was irradiated. This enabled us to simulate WC tip irradiation with the fluences as high as 10^{16} protons cm^{-2}. The results of the simulation are presented in Fig. 3. As one expects, the angular distribution of the directions of the ejected protons is symmetric around the *Y*-axis (Fig. 3(a)). In general, the angular deflection of most of the tip-ejected protons from the original beam direction is relatively small and is within about 2°. Furthermore, it is clear from Fig. 3(b), that small energy loss is more probable than a large energy loss. The fraction of ions that are transmitted after impinging on a 1 μm projected edge width of the slit is 65%. Energy loss of some 60% of these ejected protons is less than 300 keV (Fig. 3(b)). Furthermore, about 0.36% of the total fluence of the tip-scattered protons lose less than 1 keV of their energy, 0.8% – less than 2 keV, 2.2% – less than 5 keV, 4.3% – less than 10 keV, 8.6% – less than 20 keV, and 20.3% – less than 50 keV (Fig. 3(b)). Moreover, the fraction of protons that have undergone a given energy loss (ΔE_{max}) shows a straight-line dependance on ΔE_{max}. About 1% are scattered to <0.5° (9 mrad) with respect to the beam axis (Fig. 3(c) and (d)). The object slits are comprised of four WC cylindrical blades, therefore, the total fluence of the tip-scattered protons is enhanced several fold. Magnetic lens systems are momentum dispersive and hence ions that have lost a sufficiently small amount of energy, that they can be transmitted by the lenses, will contribute to the focused beam broadening. Surface degradation in the form of roughening will destroy the straight-line dependance above giving rise to an increased fraction that have undergone a small energy loss. This in turn will lead to an increase in chromatic aberration.

5. Conclusion

Using the GEANT4 toolkit various processes at the near-edge region of the apertures can be studied. In this work, we investigated the implantation profile of 2 MeV protons in the WC cylinder used in nuclear microscopy for object and scraper apertures, and scattering of 2 MeV protons from the tip of the slit.

The results indicate that long lasting irradiation of the WC cylinder results in substantial implanted concentrations at the edge further upstream from the tip of a WC cylinder. The implanted doses in the near-tip region are smaller than for more oblique incidence, but considerable. The edge erosion of the slit induced by irradiation is not likely to be caused via aggregation of the implanted hydrogen into bubbles, but rather via other mechanisms, e.g. sputtering.

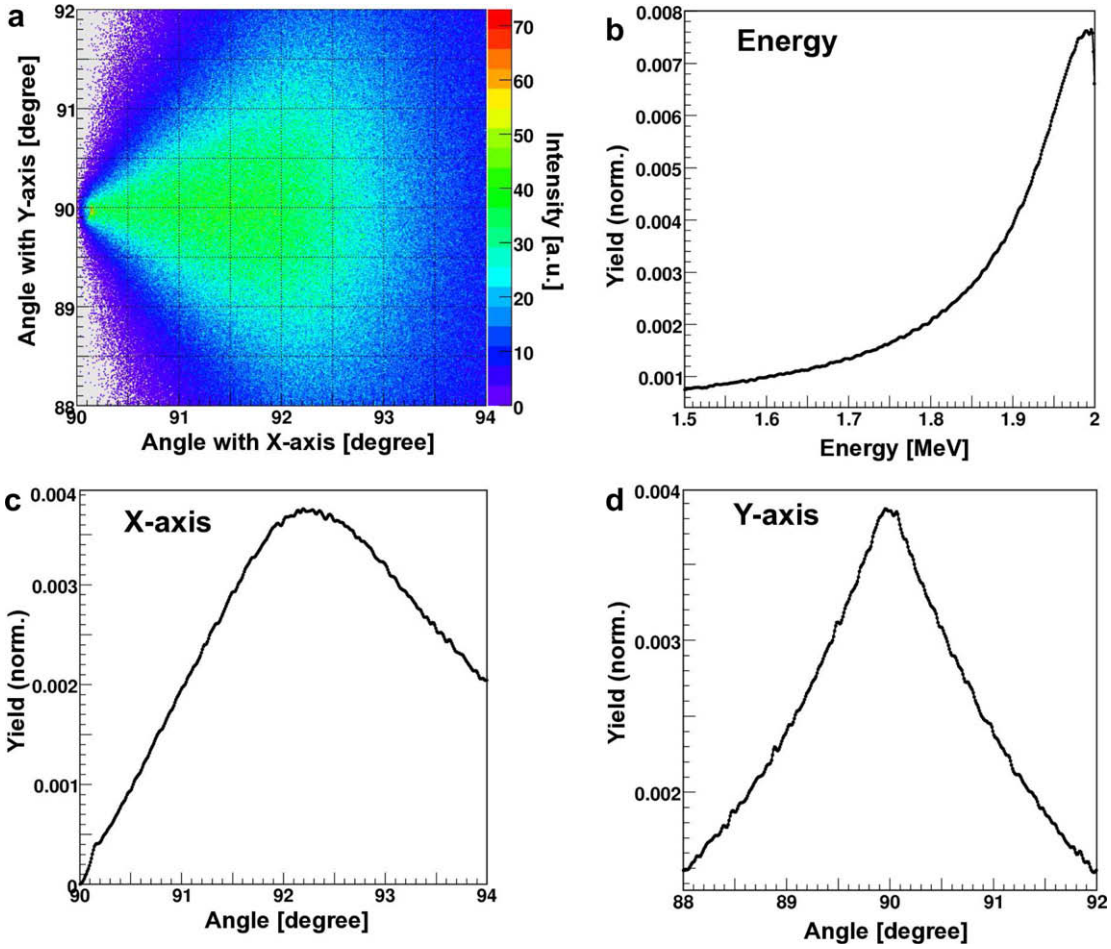


Fig. 3. Angular and energy distributions of protons scattered from the edge of the WC cylinder. The simulated fluence (number of protons per unit area that is perpendicular to the beam axis) impinging on the tip of the WC cylinder was 10^{16} protons cm^{-2}. The beam axis is along – *Z*-direction. (a) Angular distribution of edge-scattered protons. Note, that because the WC cylinder was positioned at $X > 0$ the angles between the protons' momenta and the *X*-axis are greater that 90° (see also Fig. 2(c)). (b) Energy distribution of the edge-scattered protons. (c) Angular distribution of the directions of the edge-scattered protons with respect to the *X*-axis (see also Fig. 2(a)). (d) Angular distribution of the directions of the edge-scattered protons with respect to the *Y*-axis.

Most of the tip-scattered protons are scattered into angles <2° with respect to the incident beam axis. Although 65% of the protons from the fluence incident on 1 μm edge projected width of the slit are ejected, most of these will not contribute to the beam spot broadening because large angle divergence or large change in energy implies they will not be transmitted to the target. The small fraction that have not undergone large angle scattering and small energy loss will however manifest themselves as chromatic aberrations. It follows that if surface roughening increases the fraction of ions undergoing small energy loss this will increase the chromatic aberration and degrade the beam spot.

Acknowledgements

This work has been carried out under the auspices of the Academy of Finland Centre of Excellence in Nuclear and Accelerator Based Physics (Ref. 213503). SG and HJW are both grateful for travel support from Magnus Ehrnrooth foundation. Frank Watt and Jeroen van Kan are thanked for providing the sample and helpful discussions.

References

[1] F. Watt, M.B.H. Breese, A.A. Bettiol, J.A. van Kan, Mater. Today 30 (2007) 20.
[2] J.A. van Kan, P.G. Shao, K. Ansari, A.A. Bettiol, T. Osipowicz, F. Watt, Microsyst. Technol. 13 (2007) 431.
[3] C. Michelet-Habchi, S. Incerti, P. Aguer, Ph. Barbaret, E. Gontier, T. Guinefolleau, Ph. Moretto, A. Pouthier, T. Pouthier, R.W. Smith, IEEE Trans. Nucl. Sci. 52 (2005) 612.
[4] M. Ren, J.A. van Kan, A.A. Bettiol, L. Daina, C.Y. Gek, B.B. Huat, H.J. Whitlow, T. Osipowicz, F. Watt, Nucl. Instr. and Meth. B 260 (2007) 124.
[5] R. Rajendran, M. Ren, P. Ning, B.T.K. Huat, B. Halliwell, F. Watt, Nucl. Instr. and Meth. B 260 (2007) 136.
[6] F. Watt, J.A. van Kan, I. Rajta, A.A. Bettiol, T.F. Choo, M.B.H. Breese, T. Osipowicz, Nucl. Instr. and Meth. B 210 (2003) 14.
[7] J. van Erps, B. Volckaerts, H. van Amerongen, P. Vynck, R. Krajewski, C. Debaes, J. Watte, A. Hermanne, H. Thienpont, IEEE Photon. Technol. Lett. 18 (2006) 1164.
[8] B. Volckaerts, H. Ottevaere, A. Vila, M. Muruzabal, C. Debaes, P. Vynck, P. Tuteleers, V. Baukens, A. Hermanne, I. Veretennicoff, H. Thienpont, in: Optical MEMS, 2000 IEEE/LEOS International Conference, Kauai, HI, USA, 2000, p. 103.
[9] M.L. Taylor, R.D. Franich, A. Alves, P. Reichart, D.N. Jamieson, P.N. Johnston, Nucl. Instr. and Meth. B 249 (2006) 752.
[10] M.L. Taylor, A. Alves, P. Reichart, R.D. Reichart, S. Rubanov, P. Johnston, D.N. Jamieson, Nucl. Instr. and Meth. B 260 (2007) 426.
[11] S. Gorelick, N. Puttaraksa, T. Sajavaara, M. Laitinen, S. Singkarat, H.J. Whitlow, Nucl. Instr. and Meth. B 266 (2008) 2461.
[12] N. Puttaraksa, S. Gorelick, T. Sajavaara, M. Laitinen, S. Singkarat, H.J. Whitlow, J. Vac. Sci. Technol. B 26 (2008) 1732.
[13] S. Gorelick, T. Ylimäki, T. Sajavaara, M. Laitinen, A.R.A. Sagari, H.J. Whitlow, Nucl. Instr. and Meth. B 260 (2007) 77.
[14] S. Gorelick, T. Sajavaara, H.J. Whitlow, J. Vac. Sci. Technol. B (2009), accepted for publication.
[15] S. Gorelick, T. Sajavaara, H.J. Whitlow, J. Vac. Sci. Technol. B (2009), accepted for publication.
[16] S. Agostinelli et al., Nucl. Instr. and Meth. A 506 (2003) 250.
[17] J. Allison et al., IEEE Trans. Nucl. Sci. 53 (2006) 270.
[18] GEANT4 Version 4.9.0 With Low Energy Extension G4LOWEM3.0. <http://geant4.web.cern.ch/geant4>.
[19] J.F. Ziegler, Stopping and Range of Ions in Matter (SRIM – 2006). <http://www.SRIM.org>.
[20] S. Incerti, Ph. Barbaret, B. Courtois, C. Michelet-Habchi, Ph. Moretto, Nucl. Instr. and Meth. B 210 (2003) 92.
[21] GEANT4 Physics Reference Manual. <http://geant4.web.cern.ch/geant4/UserDocumentation/UsersGuides/PhysicsReferenceManual/fo/PhysicsReferenceManual.pdf>.
[22] GEANT4 General Particle Source. <http://reat.space.qinetiq.com/gps/>.
[23] OM10 Precision Differential Micrometre Controlled Beam Defining Slits, Oxford Microbeams Ltd. <http://www.microbeams.co.uk>.